






Article

In Silico Molecular Studies of Antiophidic Properties of the Amazonian Tree *Cordia nodosa* Lam.

Carmen X. Luzuriaga-Quichimbo ¹, José Blanco-Salas ^{2,*}, Luz María Muñoz-Centeno ³, Rafael Peláez ⁴, Carlos E. Cerón-Martínez ⁵ and Trinidad Ruiz-Téllez ²

¹ Faculty of Health Sciences Eugenio Espejo, University UTE, Quito 170147, Ecuador; luzuriaga.cx@gmail.com

² Department, Faculty of Sciences, University of Extremadura, 06006 Badajoz, Spain; truíz@unex.es

³ Department of Botany, University of Salamanca, 37008 Salamanca, Spain; luzma@usal.es

⁴ Department of Pharmaceutical Sciences, Organic Chemistry, University of Salamanca, 37008 Salamanca, Spain; pelaez@usal.es

⁵ Herbarium Alfredo Paredes, QAP, Ecuador Central University UCE, Quito 170521, Ecuador; carlosceron57@hotmail.com

* Correspondence: blanco_salas@unex.es; Tel.: +34-924-289-300

Academic Editor: Ericsson Coy-Barrera

Received: 11 October 2019; Accepted: 11 November 2019; Published: 16 November 2019



Abstract: We carried out surveys on the use of *Cordia nodosa* Lam. in the jungles of Bobonaza (Ecuador). We documented this knowledge to prevent its loss under the Framework of the Convention on Biological Diversity and the Nagoya Protocol. We conducted bibliographic research and identified quercetrin as a significant bioactive molecule. We studied its in silico biological activity. The selected methodology was virtual docking experiments with the proteins responsible for the venomous action of snakes. The molecular structures of quercetrin and 21 selected toxins underwent corresponding tests with SwissDock and Chimera software. The results point to support its antiophidic use. They show reasonable geometries and a binding free energy of -7 to -10.03 kcal/mol. The most favorable values were obtained for the venom of the Asian snake *Naja atra* (5Z2G, -10.03 kcal/mol). Good results were also obtained from the venom of the Latin American *Bothrops pirajai* (3CYL, -9.71 kcal/mol) and that of Ecuadorian *Bothrops asper* snakes (5TFV, -9.47 kcal/mol) and *Bothrops atrox* (5TS5, -9.49 kcal/mol). In the 5Z2G and 5TS5 L-amino acid oxidases, quercetrin binds in a pocket adjacent to the FAD cofactor, while in the myotoxic homologues of PLA2, 3CYL and 5TFV, it joins in the hydrophobic channel formed when oligomerizing, in the first one similar to α -tocopherol. This study presents a case demonstration of the potential of bioinformatic tools in the validation process of ethnobotanical phytopharmaceuticals and how in silico methods are becoming increasingly useful for sustainable drug discovery.

Keywords: *Cordia*; in silico; antiophidic; quercetrin; docking; validation

1. Introduction

Cordia is a tropical genus of arbustive *Boraginaceae* and is quite interesting from a pharmacological point of view [1]. More than thirty species are referenced as medicinal [2], having bioactive compounds such as rosmarinic acid, cordiaquinones and cordiachromes [3,4]. *Cordia alliodora* Cham., one of the most important timber trees in the Amazon, has an interesting chemical profile [5–11] with antimicrobial, antifungal, larvicidal [12] and cytotoxic activities [13] which have been experimentally tested. *Cordia verbenaceae* DC has been studied as anti-inflammatory [14], analgesic [15], antibacterial [16], antiallergic [17] and antitumoral [18]; the latter activity is attributed to the rosmarinic acid (Figure 1) [19].

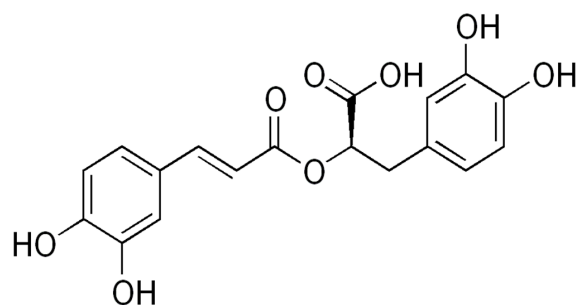


Figure 1. Rosmarinic acid.

Another *Cordia* with promising properties is *Cordia nodosa* Lam, (= *Cordia collococa* Aubl [20]) a Pan-Amazonian species that contains [13] quercetrin (Figure 2), a strong antiproliferative in vitro.

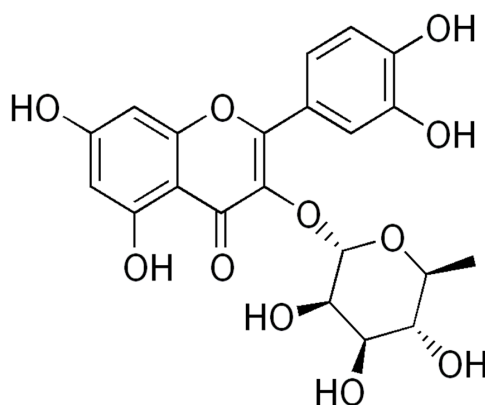


Figure 2. Quercetrin.

In Amazonian Ecuador, many ethnic groups (cofan, redwood, siona, wao, shuar, achuar and kichwa) have reported references to the ancestral use [21]. The fruit is edible, the wood is employed for the construction of their houses in the jungle, and cultural ceremonies and rites are prepared with the leaves [21]. *Cordia nodosa* Lam contains phenols that justify its anti-inflammatory and analgesic applications and its moderate bactericidal action [22]. However, the most interesting ancestral knowledge of this plant is its ability to act as an antidote to snake bites [23]. This problem, seldom considered in Europe, affects millions of inhabitants of tropical areas of the planet and has not developed a pharmaceutical research according to its dimension [24]. Every year, about 5.4 million snake bites produce 1.8–2.7 million cases of poisoning, 81,410–137,880 deaths and about three times as many amputations and other permanent disabilities [24]. The World Health Organization has included snake bites in the category of “Neglected and Forgotten Diseases” [24].

In the context of ethnobotanical research conducted by our team in the Ecuadorian Amazon [21], we carried out surveys on the use of *C. nodosa* under the Framework of the Convention on Biological Diversity and the Nagoya Protocol [25]. We had two specific aims: (a) to describe the current use as an antivenom of *C. nodosa* in the Bobonaza Basin (Pastaza, Ecuador) and (b) to offer an in silico validation by searching the scientific literature and by overall performing docking tests.

2. Results

2.1. Ethnobotanical Survey

The medicinal uses given to the species retrieved from our fieldwork prospections and literature review are summarized in Table 1, which shows that the use of *C. nodosa* as an antiophidic is currently in force in indigenous Amazonian ethnic groups. Names like kuchamanku, awas, putunmuyu, machakuymisunsal or machakuykaspi have been published previously, but not paluwapu (“= snake

stick”), which we learned from the canelo-kichwas cultures of Pastaza that we worked with [21]. We found that when a snake bite occurs, they take the bark, cook it for about one minute, and then drink the resulting liquid in a single dose.

Table 1. Medicinal uses given to the species retrieved from our fieldwork prospectations and literature review.

Organ/System	Part Used	Formulation	Traditional Knowledge	Ethnic Group-Province (Country)	Reference	
Circulatory system	leaves	decoction	hypertension	Amerindian NorthWest District (Guiana)	[26]	
Digestive system			gases	Siona-Sucumbíos (Ecuador)	[23]	
Respiratory system	bark	cooking	treat cough	Secoya-Sucumbíos (Ecuador)	[23]	
	stem					
	inner bark	finely grate and decoction	cold and shortness of breath	Amerindian (French Guiana)	[26]	
	leaves	decoction	whooping cough	Amerindian NorthWest District (Guiana)	[26]	
	fruit	suck	snot in babies	Amerindian NorthWest District (Guiana)	[26]	
Musculature and skeleton	leaves	crush the leaves and rub the body with them	rheumatism, sprains, muscle aches, bruises	Amerindian NorthWest District (Guiana)	[26]	
Nervous system and mental illness	leaves	baths with the decoction of the leaves	madness and psychiatric disorders	Yanesha (Perú)	[27]	
		decoction	headache	Amerindian NorthWest District (Guiana)	[26]	
Symptoms and states of undefined origin	bark		indeterminate conditions	Secoya-Sucumbíos (Ecuador)	[23]	
	flowers			Kichwa del Oriente-Orellana (Ecuador)		
	fruit		energizing	Wao-Orellana (Ecuador)		
	leaves	infusion	dizziness	ethnicity not specified-Napo (Ecuador)		
		decoction	fever	Amerindian NorthWest District (Guiana)	[26]	
Poisoning	leaves	apply directly in the affected place		East Kichwa-Napo and Orellana (Ecuador)	[23]	
	fruit	spider bite, to decrease inflammation and prevent gangrene				
	plant					cooking
	bark					cooking
	root					cooking
	bark	scraped and in water		East Kichwa, Shuar-Napo, Orellana, Pastaza, Sucumbios (Ecuador), Piaroa (Venezuela)	[23,26]	
		infusion				
	root	infusion				
	stem	juice				
	fruit	juice				
young leaves	chewed					
	leaves	apply directly in the affected place				

2.2. Chemical and Activity Prospection: Results of the Bibliographic Review

The main component of the extract was quercetrin, a 3 α -L-rhamnoside of quercetin. The genine has a chemical structure based on a C6-C3-C6 carbon skeleton, with a chromene ring bearing a second aromatic ring at position 2. Therefore, it is a flavonoid, specifically a flavonol (Figure 2). This is a chemical group in which antiophidic properties are known [28].

The literature review performed is summarized in the following tables. It is known that snake venom comprises peptides and proteins that act as cytotoxins, neurotoxins, hemotoxins or myotoxins. The 21 molecular targets of snakebite poisonings, retrieved from our bibliographic research, are shown in Table 2.

Table 2. Toxins from Ecuadorian (1–2), Latin American (3–13) or non-American (14–21) snakes, and the corresponding Protein Data Base Identifier (PDB ID).

Toxin	PDB ID	Reference
1. MT-I—Basic phospholipase a2 myotoxin iii	5TFV	[29]
2. LAAO—L-amino acid oxidase from <i>Bothrops atrox</i>	5TS5	[30]
3. PLA2—Phospholipase A2: Piratoxin I (myotoxic Lys49-PLA2) from <i>Bothrops pirajai</i>	3CYL	[31]
4. PLA2—Phospholipase A2: BthTX-I—Bothropstoxin I from <i>Bothrops jararacussu</i> venom/	3CXI	[31]
5. PLA2—Phospholipase A2: Myotoxin (MjTX-I) from <i>Bothrops moojeni</i>	6CE2	[32]
6. PLA2—Phospholipase A2: Bothropstoxin I (BthTX-I)	6DIK	[33]
7. svPLA2—Phospholipase A2: myotoxin II from <i>Bothrops moojeni</i>	1XXS	[34]
8. LAAO—L-amino acid oxidase from the <i>B. jararacussu</i> venom	4E0V	[35]
9. svPLA2—Acidic phospholipase A2 (BthA-I) from <i>Bothrops jararacussu</i>	1Z76	[36]
10. VRV-PL-V—Crototoxin B, the basic PLA2 from <i>Crotalus durissusterrificus</i>	2QOG	[37]
11. PLA2—Piratoxin-II (PrTx-II) - a K49 PLA2 from <i>Bothrops pirajai</i>	1QLL	[38]
12. Bothropasin, the Main Hemorrhagic Factor from <i>Bothrops jararaca</i> venom	3DSL	[39]
13. SVM-P-I snake venom metalloproteinase BaP1	2W12	[40]
14. NNH1—L-amino acid oxidase from venom of <i>Naja atra</i>	5Z2G	[41]
15. LAAO—L-amino acid oxidase from <i>Vipera ammodytes</i> venom	3KVE	[42]
16. PDE I—Phosphodiesterase (PDE) from Taiwan cobra (<i>Naja atra atra</i>) venom	5GZ4	[43]
17. VRV-PL-V—Phospholipase ACII4 from Australian King Brown Snake (<i>Pseudechis australis</i>)	3V9M	[44]
18. NN-PL-I—Phospholipase A2 from indian cobra (<i>Naja naja</i>)	1PSH	[45]
19. LAAO—L-amino acid oxidase from Agkistrodon Halys Pallas (<i>Gloydius halys</i>)	1REO	[46]
20. NNH1—Phosphodiesterase (PDE) from Taiwan cobra (<i>Naja atra atra</i>)	5GZ5	[47]
21. PLA2—Phospholipase A2 (Pla2) from <i>Naja naja</i>	1A3D	[48,49]

2.3. Docking

The liaison energies of quercetrin with the studied targets are presented in Table 3. They have been colored by groups according to their similarity to the rest of the sequences (see Supplementary Material for details). They oscillate between -10.03 kcal/mol and -7.01 kcal/mol.

Table 3. The liaison energies of quercetrin with the PDB ID studied targets.

1.	5TFV	-9.71	MT-I—Basic Phospholipase a2 Myotoxin iii
2.	5TS5	-9.47	LAAO—L-amino acid oxidase from <i>Bothrops atrox</i>
3.	3CYL	-9.49	PLA2—Phospholipase A2: Piratoxin I (myotoxic Lys49-PLA2) from <i>Bothrops pirajai</i>
4.	3CXI	-9.37	PLA2—Phospholipase A2: BthTX-I—Bothropstoxin I from <i>Bothrops jararacussu</i> venom/
5.	4GUE	-9.30	N-terminal kinase domain of RSK2 with flavonoid glycoside quercetrin
6.	6CE2	-9.19	PLA2—Phospholipase A2: Myotoxin (MjTX-I) from <i>Bothrops moojeni</i>
7.	6DIK	-9.16	PLA2—Phospholipase A2: Bothropstoxin I (BthTX-I)
8.	1XXS	-9.01	svPLA2—Phospholipase A2: myotoxin II from <i>Bothrops moojeni</i>
9.	4E0V	-8.96	LAAO—L-amino acid oxidase from the <i>B. jararacussu</i> venom
10.	1Z76	-8.56	svPLA2—Acidic phospholipase A2 (BthA-I) from <i>Bothrops jararacussu</i>
11.	2QOG	-8.32	VRV-PL-V—Crototoxin B, the basic PLA2 from <i>Crotalus durissusterrificus</i>
12.	5A4W	-8.28	AtGSTF2 from <i>Arabidopsis thaliana</i>
13.	1QLL	-8.23	PLA2—Piratoxin-II (PrTx-II) - a K49 PLA2 from <i>Bothrops pirajai</i>
14.	3DSL	-8.20	Bothropasin, the Main Hemorrhagic Factor from <i>Bothrops jararaca</i> venom.
15.	2W12	-7.71	SVM-P-I snake venom metalloproteinase BaP1

Figures 3–15 show the molecular models of the quercetrin binding with the targets of Table 3 (left) and the corresponding 2D interaction diagram generated with LigPlot + (right) [50], made with UCSF Chimera Software. Toxins are represented in golden yellow, quercetrin in blue, and original ligands in pink. The small squares (a) show the toxin-quercetrin complex in the most favorable arrangement. When it occupies the hollow of another ligand present in the structure of the target, it has been preserved (shown as thin sticks in pink) to allow a comparison. The augmented figures (b) show, in detail, the dispositions of the quercetrin molecule between the chains of the toxins.

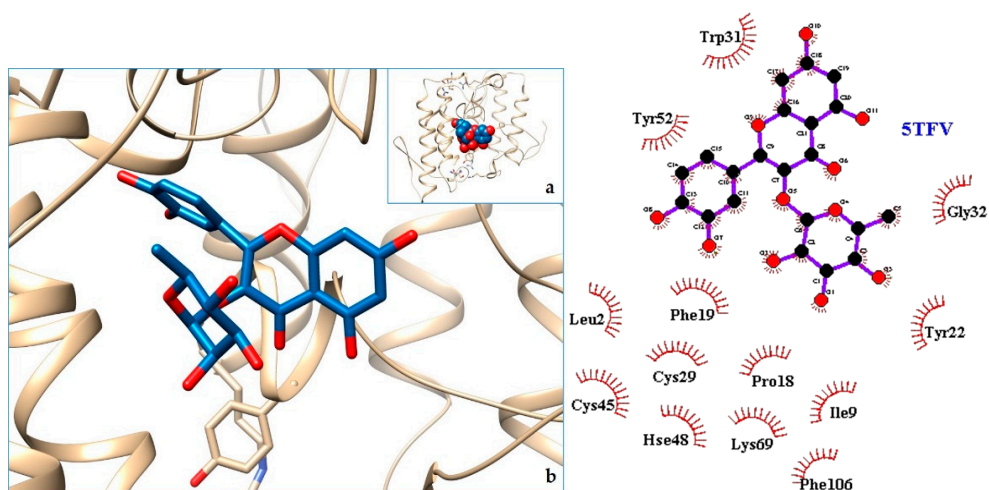


Figure 3. 5TFV-quercetrin complex. in the most favourable arrangement (a) and augmented (b) showing the disposition between the chain of toxins. Right: 2D interaction diagram.

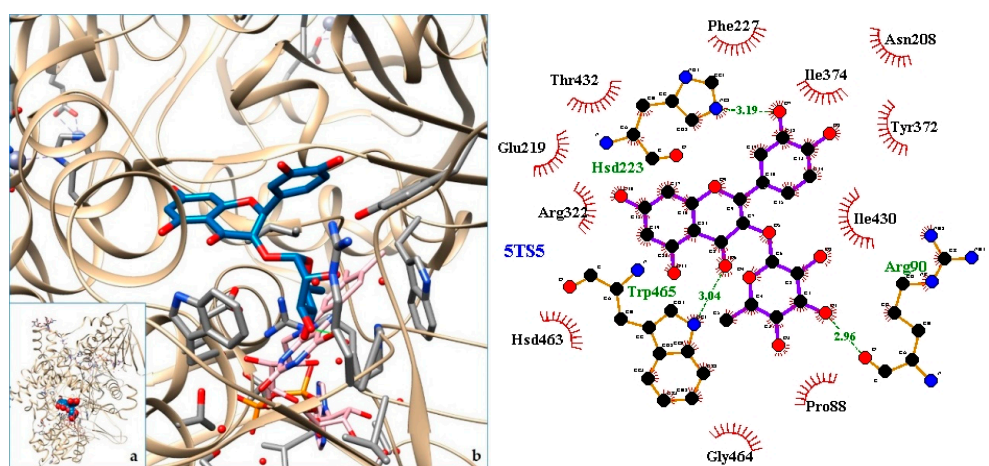


Figure 4. 5TS5-quercetrin complex. in the most favourable arrangement (a) and augmented (b) showing the disposition between the chain of toxins. Right: 2D interaction diagram.

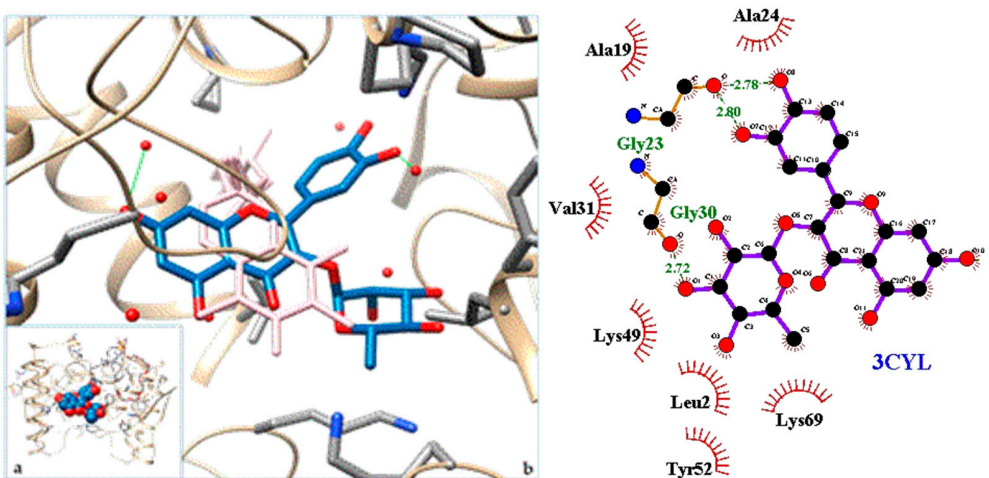


Figure 5. 3CYL quercetrin complex in the most favourable arrangement (a) and augmented (b) showing the disposition between the chain of toxins. Right: 2D interaction diagram.

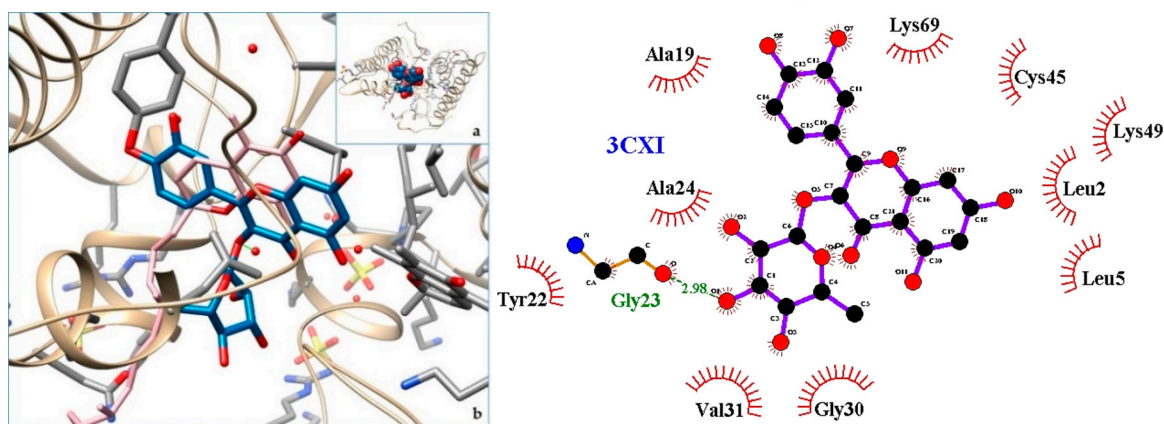


Figure 6. 3CXI-quercetin complex in the most favourable arrangement (a) and augmented (b) showing the disposition between the chain of toxins. Right: 2D interaction diagram.

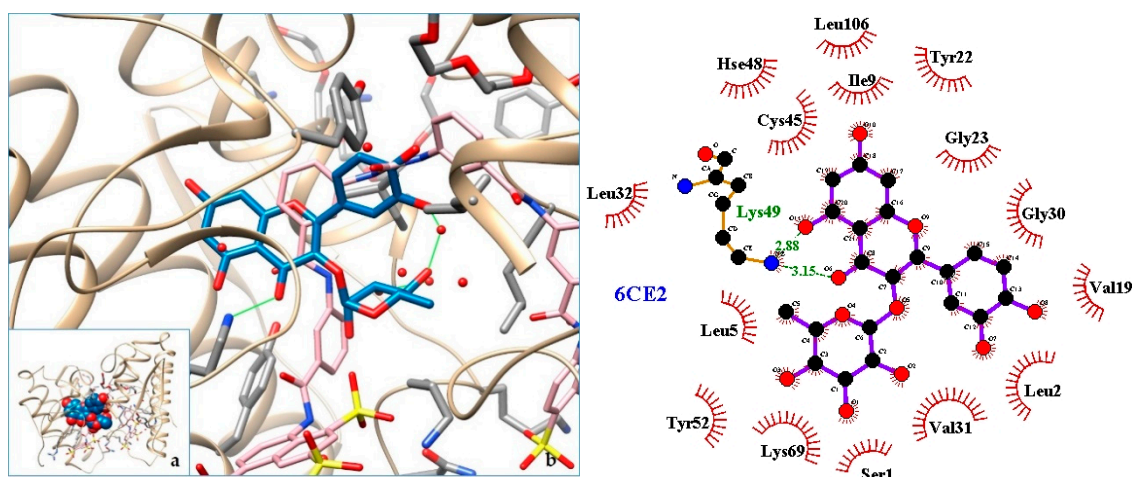


Figure 7. 6CE2-quercetin complex in the most favourable arrangement (a) and augmented (b) showing the disposition between the chain of toxins. Right: 2D interaction diagram.

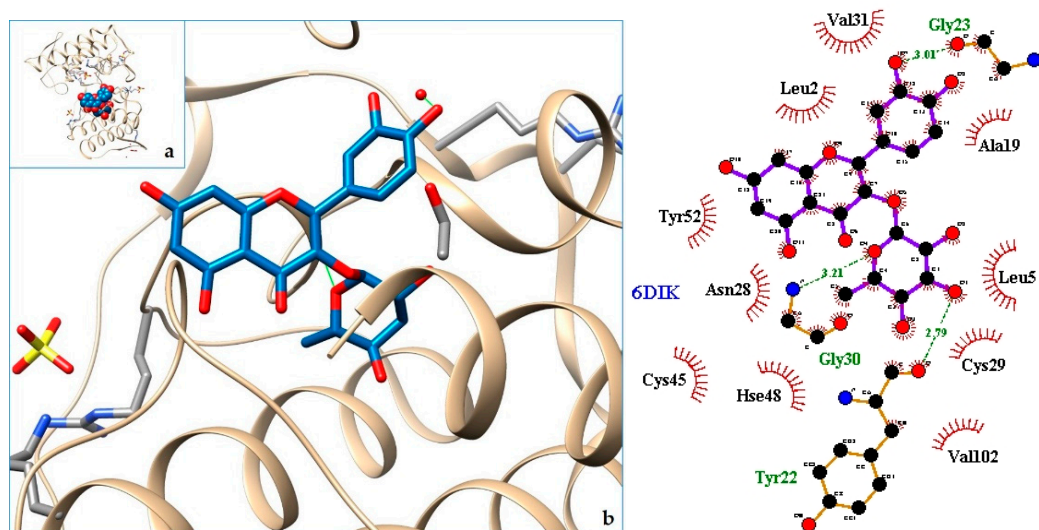


Figure 8. 6DIK-quercetin complex in the most favourable arrangement (a) and augmented (b) showing the disposition between the chain of toxins. Right: 2D interaction diagram.

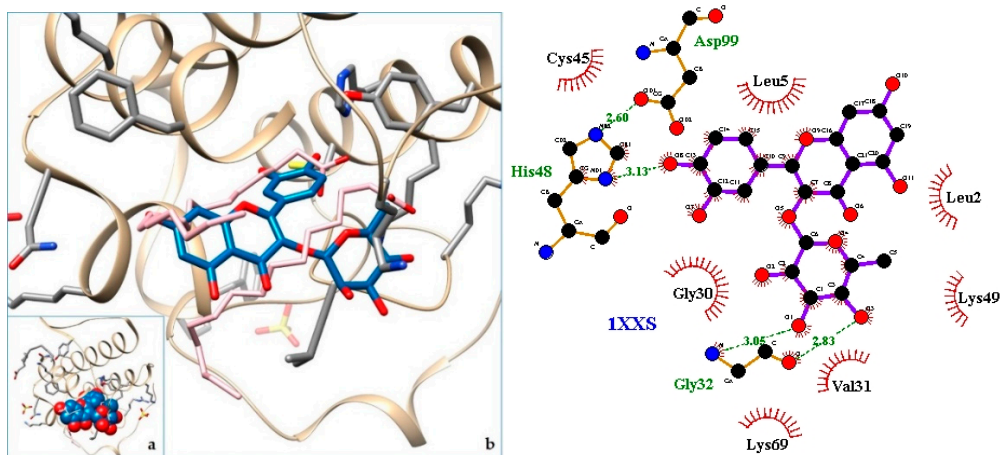


Figure 9. 1XXS-quercetrin complex in the most favourable arrangement (a) and augmented (b) showing the disposition between the chain of toxins. Right: 2D interaction diagram.

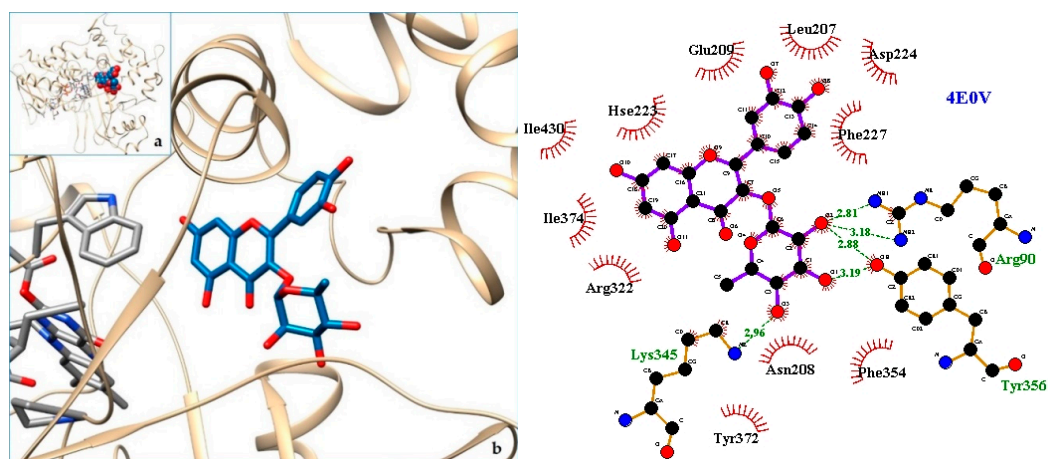


Figure 10. 4E0V-quercetrin complex in the most favourable arrangement (a) and augmented (b) showing the disposition between the chain of toxins. Right: 2D interaction diagram.

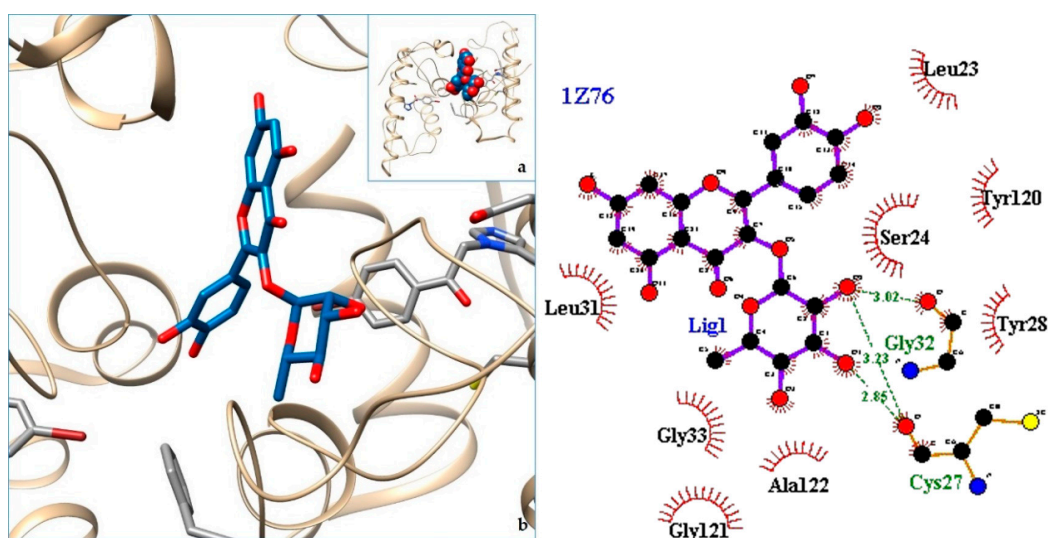


Figure 11. 1Z76-quercetrin complex in the most favourable arrangement (a) and augmented (b) showing the disposition between the chain of toxins. Right: 2D interaction diagram.

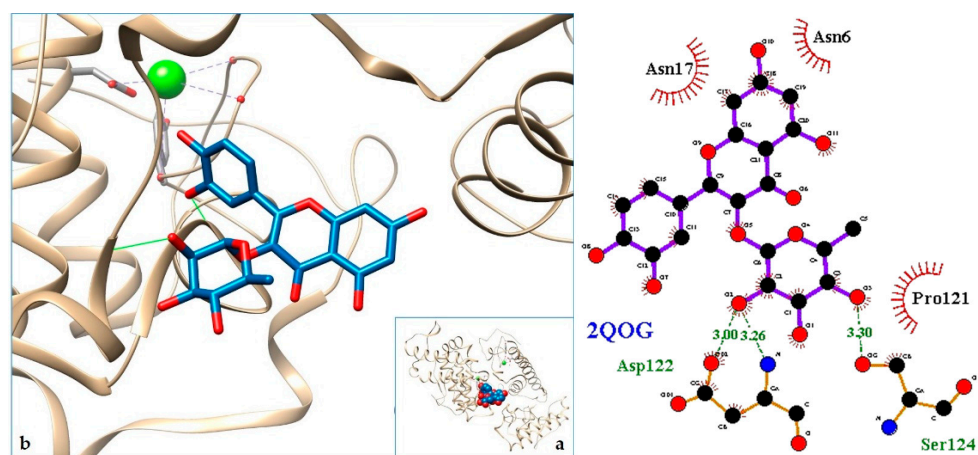


Figure 12. 2QOG-quercetrin complex in the most favourable arrangement (a) and augmented (b) showing the disposition between the chain of toxins. Right: 2D interaction diagram.

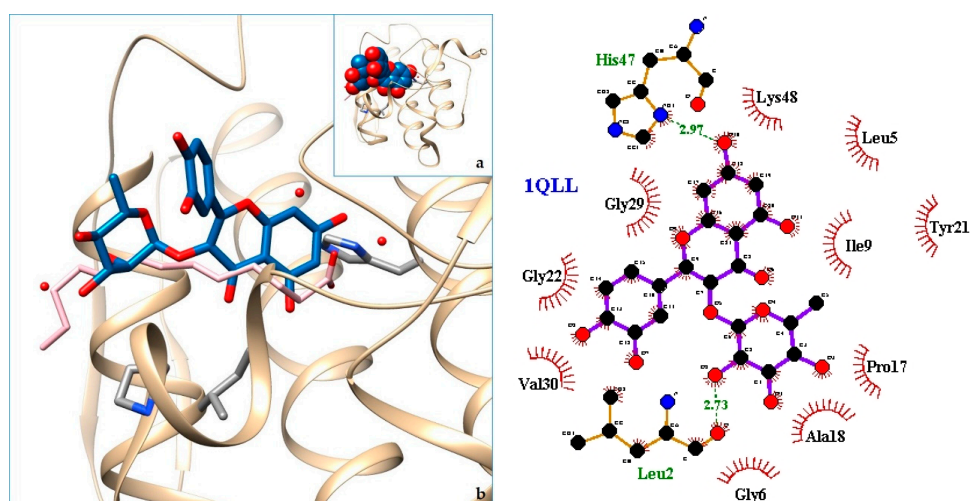


Figure 13. 1QLL-quercetrin complex in the most favourable arrangement (a) and augmented (b) showing the disposition between the chain of toxins. Right: 2D interaction diagram.

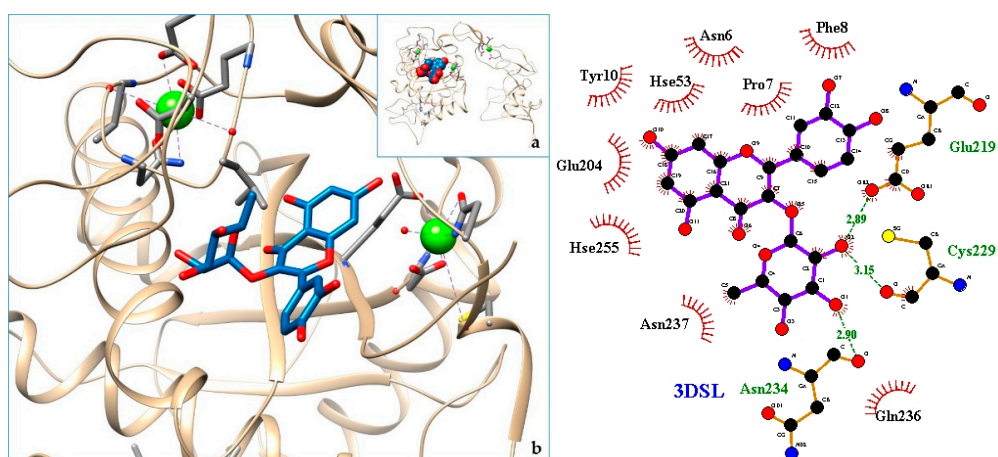


Figure 14. 3DSL-quercetrin complex in the most favourable arrangement (a) and augmented (b) showing the disposition between the chain of toxins. Right: 2D interaction diagram.

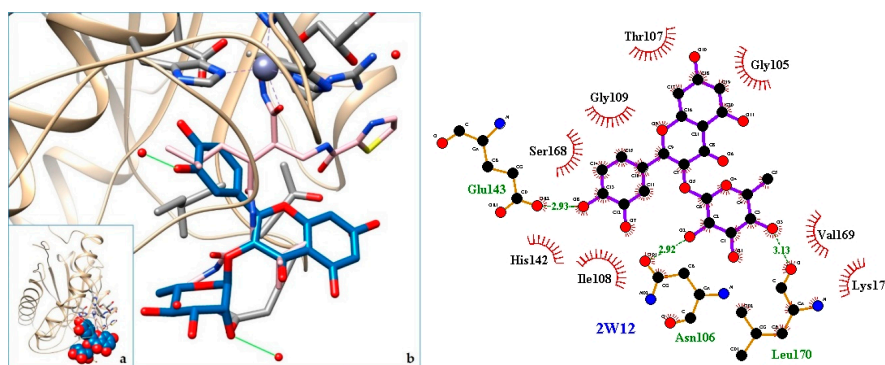


Figure 15. 2W12-quercetrin complex in the most favourable arrangement (a) and augmented (b) showing the disposition between the chain of toxins. Right: 2D interaction diagram.

3. Discussion

The traditional use of this plant for its antiophidic properties has been previously documented by the Shuar and the Napo-Rune people of neighboring provinces, although the method of application is different. In these cases, the plant is applied directly to the affected place, or they chew the young leaves and the fruits. They also prepare infusions, not with the bark, but with the root or the juice of the stem [23]. Published references on the activity of quercetrin have indicated that it inhibits lipoyxygenase svPLA2 [51] and hyaluronidase NNH1 [52], neutralizing the hemorrhagic venom of *Bothrops jararaca* [51–53], a Latin American snake.

In the docking tests that we carried out, the toxic snakes studied showed very high affinities with quercetrin. There were formed complexes of energy comparable to the ones with original targets such as 4GEW or 5A4W. Detailed information about these protein homologies has been included in Appendix A (Table A1). Thus, reasonable binding free energy values of -7 to -10 kcal/mol were obtained. The most favorable values were for the venom of the Asian snake (Chinese cobra or Taiwan cobra) *Naja atra* (5Z2G, -10.03 kcal/mol) and the Latin American *Bothrops pirajai* (3CYL, -9.71 kcal/mol). Very good results were also found with the 5TFV of the Ecuadorian snakes *Bothrops asper*, ($\Delta G -9.47$ kcal/mol) and 5TS5 of *Bothrops atrox* ($\Delta G -9.49$ kcal/mol). Therefore, quercetrin can not only be used as an antiophid for Ecuadorian venomous snakes, but for many others.

The action can be expected to be effective, especially because, in addition, the models have not presented unfavorable interactions according to SwissDock scoring terms. On many occasions, the quercetrin molecule is placed in pockets that occupy other known ligands of the targets used in this study. This is the case for 3CYL and 3CXI (Figures 5b and 6b), which occupy the pocket of α -tocopherol, 5TS5 (Figure 4b), which is close to that of FAD, 6CE2 (Figure 7b), that occupies that of suramin (a known inhibitor), 1XXS (Figure 9b), that of two stearic acids, 1QLL (Figure 13b), that of tridecanoic acid, and 2W12 (Figure 15b), which occupies the peptidomimetic inhibitor site. All of this reinforces the validity of the results of the performed docking tests.

In the 5Z2G and 5TS5 L-amino acid oxidases, quercetrin binds in a pocket adjacent to the FAD cofactor, while in the myotoxic homologues of PLA2, 3CYL and 5TFV, it joins in the hydrophobic channel formed when oligomerizing in the first one, similar to α -tocopherol.

These facts reinforce the validity of the traditional use reported. They will have to be corroborated in vitro, in vivo, and even with subsequent clinical trials. Nevertheless, this is encouraging evidence in the field of finding new solutions to this pathology.

4. Materials and Methods

4.1. Ethnobotanical Survey

All the information referring to the ethnobotanical study from which the data derives is available in Appendix A, which contains references to voucher specimens, authorizations and permissions.

Table 1 summarizes the medicinal uses of the species retrieved from our fieldwork prospections and literature data.

4.2. Chemical and Activity Prospection: Bibliographic Review

A bibliographic review was carried out following the PRISMA Group method [54]. The databases accessed were Academic Search Complete, Agricola, Agris, Biosis, CABS, Cochrane, Cybertesis, Dialnet, Directory of Open Access Journals, Embase, Espacenet, Google Patents, Google Academics, Medline, PubMed, Science Direct, Scopus, Teseo, and ISI Web of Science. The selected citations were summarized, and a critical reading allowed us to develop the discussion.

4.3. Docking

The molecular docking method applied comprises the following procedures: ligand preparation, protein selection, docking, and analysis of the results. The energies produced after docking, interaction residues and interaction types were studied for the analyses following general procedure for molecular docking [55,56]. Docking was performed with the SwissDock Docking Web Service (Available online: <http://www.loc.gov>). A 3D quercetrin virtual structure was built with Spartan[®], Wavefunction Inc. Selection of targets was made based on a bibliographic review of natural bioactive compounds against snake bites [28,54]. A total of 21 venoms from snakes (targets) with known X-ray structures were tested (see Table 2, Table 3 and Supplementary Material). Molecular structures were consulted in the Protein Data Bank (PDB), and the reference IDs were taken to include them in the Swiss Dock Program. The target + ligand set was considered stable when the values of the binding free energy were lower than -7 kcal/mol. This consideration is based on docking experiments with the known X-ray structures 4GUE and 5A4W complexes of quercetrin resulting in binding energies values of -9.30 and -8.28 kcal/mol, respectively. Once the results of the docking were obtained, they were analyzed with UCSF Chimera.

5. Conclusions

The information obtained from the ethnobotanical investigations carried out in the Bobonaza Basin (Ecuador) allowed us to verify the good capacity *in silico* of quercetrin, the active ingredient obtained from *Cordia nodosa*. The binding energies of quercetrin with all the macromolecules (toxins from venoms of different snakes) were adequate, since they were all less than -7 kcal/mol.

The *in silico* docking evaluation combined with ethnobotanical information was very effective as a research method. It allowed us to select the appropriate active principle from the beginning, thus avoiding the tedious previous work of testing principle assets that have no references and therefore working blindly with molecules that would not couple to these toxins. The search for new bio-products oriented from basic ethnobotanical knowledge is an investigation that could result in products with great therapeutic efficacies.

Supplementary Materials: The following are available online at <http://www.mdpi.com/1420-3049/24/22/4160/s1>, Table S1: Similarity matrix for the target proteins. Table S2: Heat map of sequence similarities as indicated in Table S1.

Author Contributions: Conceptualization T.R.-T. methodology, C.E.C.-M. and C.X.L.-Q.; validation J.B.-S.; formal analysis, R.P. and L.M.M.-C.; investigation, C.X.L.-Q.; data curation, C.E.C.-M. and C.X.L.-Q.; writing—original draft preparation, T.R.-T.; writing—review and editing, J.B.-S., R.P. and L.M.M.-C.; visualization, L.M.M.-C. and R.P.; supervision, C.X.L.-Q.; project administration, T.R.-T.; funding acquisition, C.X.L.-Q., J.B.-S. and T.R.-T.

Funding: This research was partially funded by the Government of Extremadura (Spain) and the European Union through the action “Apoyos a los Planes de Actuación de los Grupos de Investigación Catalogados de la Junta de Extremadura: FEDER GR18169.

Acknowledgments: We are grateful to the members of the Kichwa community of Pakayaku, Ms. Luzmila Gayas, the People’s Assembly of Pakayaku and the collaborating *ayllus* (families), for their cooperation during the field work. F. Centeno Velázquez, D. Morales Jadan (University of Extremadura), collaborated actively in the improvement of the original manuscript.

Conflicts of Interest: The authors declare no conflict of interest. The founding sponsors had no role in the design of the study; in the collection, analyses, or interpretation of data; in the writing of the manuscript, and in the decision to publish the results.

Abbreviations

PDB ID	Toxin
4GUE	N-terminal kinase domain of RSK2
5A4W	AtGSTF2 from <i>Arabidopsis thaliana</i>
3CYL	PLA2—Phospholipase A2: Piratoxin I (myotoxic Lys49-PLA2) from <i>Bothrops pirajai</i>
5TFV	MT-I—Basic phospholipase a2 myotoxin iii
5TS5	LAAO—L-amino acid oxidase from <i>Bothrops atrox</i>
3CXI	PLA2—Phospholipase A2: BthTX-I—Bothropstoxin I from <i>Bothrops jararacussu</i> venom/
6CE2	PLA2—Phospholipase A2: Myotoxin (MjTX-I) from <i>Bothrops moojeni</i>
6DIK	PLA2—Phospholipase A2: Bothropstoxin I (BthTX-I)
1XXS	svPLA2—Phospholipase A2: myotoxin II from <i>Bothrops moojeni</i>
4E0V	LAAO—L-amino acid oxidase from the <i>Bothrops jararacussu</i> venom
1Z76	svPLA2—Acidic phospholipase A2 (BthA-I) from <i>Bothrops jararacussu</i>
2QOG	VRV-PL-V—Crototoxin B, the basic PLA2 from <i>Crotalus durissus terrificus</i>
1QLL	PLA2—Piratoxin-II (Prtx-II) - a K49 PLA2 from <i>Bothrops pirajai</i>
3DSL	Bothropasin, the Main Hemorrhagic Factor from <i>Bothrops jararaca</i> venom.
2W12	SVMP—P-I snake venom metalloproteinase BaP1
5Z2G	NNH1—L-amino acid oxidase from venom of <i>Naja atra</i>
3KVE	LAAO—L-amino acid oxidase from <i>Vipera ammodytes</i> venom
5GZ4	PDE I—Phosphodiesterase (PDE) from Taiwan cobra (<i>Naja atra atra</i>) venom
3V9M	VRV-PL-V—Phospholipase ACII4 from Australian King Brown Snake (<i>Pseudechis australis</i>)
1PSH	NN-PL-I—Phospholipase A2 from indian cobra (<i>Naja naja</i>)
1REO	LAAO—L-amino acid oxidase from Agkistrodon Halys Pallas (<i>Gloydius halys</i>)
5GZ5	NNH1—Phosphodiesterase (PDE) from Taiwan cobra (<i>Naja atra atra</i>)
1A3D	PLA2—Phospholipase A2 (Pla2) from <i>Naja naja</i>

Appendix A

The Kichwa community of Pakayaku (Bobonaza River, Pastaza, Ecuador) lies in a fairly isolated region where bio- and ethno-diversity studies are still lacking. One of us (CXLQ) was based in the Biological Station PindoMirador in the northern Bobonaza River basin (S1°27'09"-W 78°04'51"), and since 2008 was in charge of environmental monitoring and education programs involving the local population.

Permissions and Authorizations/Ethnobotanical Survey: Under the Protocol of Nagoye (CBD, 2010) collective written research consent was granted by Mrs. Luzmila Gayas, the community president of the Assembly of Pakayaku. Permissions for collecting and moving plant material (MAE-DPAP-2016-2243) was granted by the Ministry of Environment of Ecuador. Prior verbal individual consents were obtained from the persons taking part in our survey. Our investigation consisted of a series of planned residential visits and treks accompanied by Kichwa interpreters and the local inhabitants of Pakayaku.

Vouchers: Sheets at Herbarium Alberto José Paredes, Universidad Central de Ecuador, Quito (QAP). Ecuador, Pastaza: Pakayaku, banks of the Bobonaza River, sector of Yanalpa, chacra n° 6 belonging to Mr. Aparicio Aranda, two hours walking away from the community, 592 m, 01°39'03" S, 077°34'36" W, lowland evergreen forest, 23 January 2016, C. X. Luzuriaga-Q & R. Aranda (QAP 92888); sector of Aychatambo, banks of the Bobonaza River, upstream by canoe, twenty minutes away from the community, 425 m, 01°37'51.8" S, 077°36'31.4" W, lowland evergreen forest, 27 November 2015, C. X. Luzuriaga-Q & L. Gayas (QAP 92547). Material identified by C. Cerón Martínez.

Interviews: They were semi-structured and included a series of open questions aimed to encourage discussion. Knowledgeable elders of the Pakayaku community acted as informants and agreed to reveal their knowledge on the species and to be recorded. The informants answered freely on several topics, including the common name of Kichwa, part of the plant used, description of usage, harvest season, storage (if any), preparation of concoction, and the target of the treatment.

Informatization: After the fieldwork, the data were included into an MS Excel spreadsheet. All the uses recorded were classified according to the classification scheme proposed by [21], which is in turn based on the report of De la Torre and coworkers [23]. *Cordia nodosa* data are included in Table 1.

Table A1. Similarity matrix for the target proteins. In each cell the upper number represents the percentage of identity and the lower the percentage of similarity for the protein in that row. The number in parenthesis represent the corresponding amino-acid number after Smith-Waterman comparison of the sequences. The cells are colored according to the percentage of similarity: <25% yellow, 25–50% orange, 50–75% green and >75% light blue. Diagonal cells with 100% identity are colored in dark blue. The protein IDs in the upper row have been colored by groups according to their similarity to the rest of the sequences.

	4GUE (305)	5A4W (212)	1QLL (121)	1XXS (122)	1Z76 (123)	2QOG (122)	2W12 (202)	3CXI (121)	3CYL (121)	3DSL (419)	4E0V (497)	5TFV (122)	5TS5 (484)	6CE2 (121)	6DIK (121)
4GUE (305)	100%	2.95% (9) 5.25% (16)	1.64% (5) 2.30% (7)	1.64% (5) 2.95% (9)	1.97% (6) 1.97% (6)	1.31% (4) 1.31% (4)	8.20% (25) 14.10% (43)	1.97% (6) 2.95% (9)	1.64% (5) 2.30% (7)	5.90% (18) 8.20% (25)	8.52% (26) 16.07% (49)	1.97% (6) 3.28% (10)	6.23% (19) 13.77% (42)	1.31% (4) 1.64% (5)	1.97% (6) 2.95% (9)
5A4W (212)	4.25% (9) 7.55% (16)	100	2.36% (5) 2.83% (6)	2.83% (6) 4.72% (10)	2.83% (6) 4.25% (9)	3.77% (8) 4.25% (9)	6.60% (14) 9.91% (21)	2.36% (5) 2.83% (6)	2.62% (13) 3.43% (17)	4.25% (9) 8.49% (18)	19.81% (42) 35.38% (75)	2.36% (5) 2.83% (6)	19.81% (42) 35.38% (75)	5.19% (11) 6.60% (14)	2.36% (5) 2.83% (6)
1QLL (121)	4.13% (5) 5.79% (7)	4.13% (5) 4.96% (6)	100%	93.39% (113) 95.04% (115)	48.76% (59) 70.25% (85)	48.76% (59) 62.81% (76)	4.96% (6) 7.44% (9)	98.35% (119) 99.17% (120)	99.17% (120) 99.17% (120)	14.05% (17) 21.49% (26)	19.83% (24) 35.54% (43)	60.33% (73) 71.07% (86)	5.79% (7) 9.09% (11)	86.78% (105) 89.26% (108)	99.17% (120) 99.17% (120)
1XXS (122)	4.10% (5) 7.38% (9)	4.92% (6) 8.20% (10)	92.62% (113) 94.26% (115)	100%	50.82% (62) 69.67% (85)	49.18% (60) 63.11% (77)	4.92% (6) 7.38% (9)	94.26% (115) 95.08% (116)	92.62% (113) 94.26% (115)	13.93% (17) 21.31% (26)	9.84% (12) 16.39% (20)	59.84% (73) 69.67% (85)	4.10% (5) 5.74% (7)	82.79% (101) 85.25% (104)	93.44% (114) 95.08% (116)
1Z76 (122)	4.92% (6) 4.92% (6)	4.92% (6) 7.38% (9)	48.36% (59) 69.67% (85)	50.82% (62) 69.67% (85)	100%	56.56% (69) 66.39% (81)	7.38% (9) 9.02% (11)	50.0% (61) 70.49% (86)	48.36% (59) 69.67% (85)	18.85% (23) 28.69% (35)	8.20% (19) 9.02% (11)	56.56% (69) 71.31% (87)	8.20% (10) 9.84% (12)	50.00% (61) 65.57% (80)	49.18% (60) 70.49% (86)
2QOG (122)	3.28% (4) 3.28% (4)	6.56% (8) 7.38% (9)	48.36% (59) 62.30% (76)	49.18% (60) 63.11% (77)	56.56% (69) 66.39% (81)	100%	7.38% (9) 10.66% (13)	47.54% (58) 62.30% (76)	48.36% (59) 62.30% (76)	22.13% (27) 28.69% (35)	9.84% (12) 18.03% (22)	63.93% (78) 76.23% (93)	9.84% (12) 18.03% (22)	47.54% (58) 57.38% (70)	48.36% (59) 62.30% (76)
2W12 (202)	12.38% (25) 21.29% (43)	6.93% (14) 10.40% (21)	2.97% (6) 4.46% (9)	2.97% (6) 4.46% (9)	4.46% (9) 5.45% (11)	4.46% (9) 6.44% (13)	100%	2.97% (6) 4.46% (9)	2.97% (6) 4.46% (9)	52.48% (106) 67.82% (137)	3.47% (7) 5.45% (11)	1.98% (4) 2.97% (6)	3.47% (7) 5.45% (11)	7.92% (16) 12.87% (26)	2.97% (6) 4.46% (9)
3CXI (121)	4.96% (6) 7.44% (9)	4.13% (5) 4.96% (6)	98.35% (119) 99.17% (120)	95.04% (115) 95.87% (116)	50.41% (61) 71.07% (86)	47.93% (58) 62.81% (76)	4.96% (6) 7.44% (9)	100%	98.35% (119) 99.17% (120)	14.05% (17) 21.49% (26)	19.83% (24) 34.71% (42)	59.50% (72) 70.25% (85)	5.79% (7) 9.09% (11)	85.95% (104) 89.26% (108)	99.17% (120) 100% (122)
3CYL (121)	4.13% (5) 5.79% (7)	10.74% (13) 14.05% (17)	99.17% (120) 99.17% (120)	93.39% (113) 95.04% (115)	48.76% (59) 70.25% (85)	48.76% (59) 62.81% (76)	4.96% (6) 7.44% (9)	98.35% (119) 99.17% (120)	100%	14.05% (17) 21.49% (26)	19.83% (24) 35.54% (43)	59.50% (72) 70.25% (85)	5.79% (7) 9.09% (11)	87.60% (106) 90.08% (109)	99.17% (120) 99.17% (120)
3DSL (479)	4.30% (18) 5.97% (25)	2.15% (9) 4.30% (18)	4.06% (17) 6.21% (26)	4.06% (26) 6.21% (26)	5.49% (23) 8.35% (35)	6.44% (35) 8.35% (35)	25.30% (106) 32.70% (137)	4.06% (17) 6.21% (26)	4.06% (17) 6.21% (26)	100%	2.39% (10) 3.34% (14)	4.06% (17) 5.97% (25)	2.39% (10) 3.58% (15)	4.06% (17) 6.68% (28)	4.06% (17) 6.21% (26)
4E0V (497)	5.23% (26) 9.86% (49)	8.45% (42) 15.09% (75)	4.83% (24) 8.65% (43)	2.41% (12) 4.02% (20)	2.01% (19) 2.21% (11)	2.41% (12) 4.43% (22)	1.41% (7) 2.21% (11)	4.83% (24) 8.45% (42)	4.83% (24) 8.65% (43)	2.01% (10) 2.82% (14)	100%	3.22% (16) 5.63% (28)	95.37% (474) 95.98% (477)	2.41% (12) 4.23% (21)	4.83% (24) 8.65% (43)
5TFV (122)	4.92% (6) 8.20% (10)	4.10% (5) 4.92% (6)	59.84% (73) 70.49% (86)	59.84% (73) 69.67% (85)	56.56% (69) 71.31% (87)	63.93% (78) 76.23% (93)	3.28% (4) 4.92% (6)	59.02% (72) 69.67% (85)	59.02% (72) 69.67% (85)	13.93% (17) 20.49% (25)	13.11% (16) 22.95% (28)	100%	13.11% (16) 22.95% (28)	56.56% (69) 66.39% (81)	59.02% (72) 69.67% (85)
5TS5 (484)	3.93% (19) 8.68% (42)	8.68% (42) 15.50% (75)	1.45% (7) 2.27% (11)	1.03% (5) 1.45% (7)	2.07% (10) 2.48% (12)	2.48% (12) 4.55% (22)	1.45% (7) 2.27% (11)	1.45% (7) 2.27% (11)	1.45% (7) 2.27% (11)	2.07% (10) 3.10% (15)	97.93% (474) 98.55% (477)	3.31% (16) 5.79% (28)	100%	2.48% (12) 4.34% (21)	1.45% (7) 2.27% (11)
6CE2 (121)	3.31% (4) 4.13% (5)	9.09% (11) 11.57% (14)	86.78% (105) 89.26% (108)	83.47% (101) 85.95% (104)	50.41% (61) 66.12% (80)	47.93% (58) 57.85% (70)	13.22% (16) 21.49% (26)	85.95% (104) 89.26% (108)	87.60% (106) 90.08% (109)	14.05% (17) 23.14% (28)	9.92% (12) 17.36% (21)	57.02% (69) 66.94% (81)	9.92% (12) 17.36% (21)	100%	86.78% (105) 89.26% (108)
6DIK (121)	4.96% (6) 7.44% (9)	4.13% (5) 4.96% (6)	99.17% (120) 99.17% (120)	94.21% (114) 95.87% (116)	49.59% (60) 71.07% (86)	48.76% (59) 62.81% (76)	4.96% (6) 7.44% (9)	99.17% (120) 100% (122)	99.17% (120) 99.17% (120)	14.05% (17) 21.49% (26)	19.83% (43) 35.54% (43)	59.50% (72) 70.25% (85)	5.79% (7) 9.09% (11)	86.78% (105) 89.26% (108)	100%

References

1. Thirupathi, K.; Kumar, S.S.; Raju, V.S.; Ravikumar, B.; Krishna, D.R.; Mohan, G.K. A review of medicinal plants of the genus *Cordia*: Their chemistry and pharmacological uses. *J. Nat. Remedies* **2008**, *8*, 1–10.
2. Matias, E.F.F.; Alves, E.F.; do Nascimento Silva, M.K.; de Alencar Carvalho, V.R.; Coutinh, H.D.M.; da Costa, J.G.M. The genus *Cordia*: Botanists, ethno, chemical and pharmacological aspects. *Brazilian J. Pharmacogn.* **2015**, *25*, 542–552. [[CrossRef](#)]
3. Moir, M.; Thomson, R.H.; Hausen, B.M.; Simatupang, M.H. Cordiachromes: A new group of terpenoid quinones from *Cordia* spp. *J. Chem. Soc. Chem. Commun.* **1972**, *6*, 363–364. [[CrossRef](#)]
4. Moir, M.; Thomson, R.H. Naturally occurring quinones. Part XXII. Terpenoid quinones in *Cordia* spp. *J. Chem. Soc. Perkin Trans. 1* **1973**, 1352–1357. [[CrossRef](#)]
5. Kaur, S.; Singh, V.; Kumar, G.; Kad, G.L.; Singh, J. A short and facile synthesis of 2-(1Z)-(3-hydroxy-3,7-dimethylocta-1,6-dienyl)-1,4-benzenediol and 1-(3'-methoxypropanoyl)-2,4,5-trimethoxybenzene isolated from *Cordia alliodora*. *Nat. Prod. Res.* **2010**, *24*, 440–447. [[CrossRef](#)]
6. Sinha, A.K.; Joshi, B.P.; Sharma, A.; Kumar, J.K.; Kaul, V.K. Microwave-assisted rapid synthesis of methyl 2,4,5-trimethoxyphenylpropionate, a metabolite of *Cordia alliodora*. *Nat. Prod. Res.* **2003**, *17*, 419–422. [[CrossRef](#)]
7. Stevens, K.L.; Jurd, L.; Manners, G. Alliodorin, a phenolic terpenoid from *Cordia alliodora*. *Tetrahedron Lett.* **1973**, *14*, 2955–2958. [[CrossRef](#)]
8. Chen, T.K.; Ales, D.C.; Baenziger, N.C.; Wiemer, D.F. Ant-Repellent Triterpenoids from *Cordia alliodora*. *J. Org. Chem.* **1983**, *48*, 3525–3531. [[CrossRef](#)]
9. Kahn, P.H.; Cossy, J. A short synthesis of cordiachromene. *Tetrahedron Lett.* **1999**, *40*, 8113–8114. [[CrossRef](#)]
10. Bouzbouz, S.; Goujon, J.-Y.; Deplanne, J.; Kirschleger, B. Enantioselective Synthesis of Cordiachromene. *Eur. J. Org. Chem.* **2000**, *2000*, 3223–3228. [[CrossRef](#)]
11. Gary Manners, B.D.; Jurd, L.; Southwell, C.K.; Bultman, J.D.; Moir, M.; Thomson, R.H.; Perkin, J. The Hydroquinone Terpenoids of *Cordia alliodora*. *J. Chem. Soc. Perkin Trans.* **1976**, *1*, 405–410. [[CrossRef](#)]
12. Ioset, J.R.; Marston, A.; Gupta, M.P.; Hostettmann, K. Antifungal and larvicidal compounds from the root bark of *Cordia alliodora*. *J. Nat. Prod.* **2000**, *63*, 424–426. [[CrossRef](#)]
13. Fouseki, M.M.; Damianakos, H.; Karikas, G.A.; Roussakis, C.; Gupta, M.P.; Chinou, I. Chemical constituents from *Cordia alliodora* and *C. collococca* (Boraginaceae) and their biological activities. *Fitoterapia* **2016**, *15*, 9–14. [[CrossRef](#)]
14. Matias, E.F.F.; Alves, E.F.; Silva, M.K.N.; Carvalho, V.R.A.; Figueredo, F.G.; Ferreira, J.V.A.; Coutinho, H.D.M.; Silva, J.M.F.L.; Ribeiro-Filho, J.; Costa, J.G.M. Seasonal variation, chemical composition and biological activity of the essential oil of *Cordia verbenacea* DC (Boraginaceae) and the sabinene. *Ind. Crops Prod.* **2016**, *87*, 45–53. [[CrossRef](#)]
15. De Alencar Carvalho, V.R.; do Nascimento Silva, M.K.; Aguiar, J.J.S.; de Carvalho Nilo Bitu, V.; da Costa, J.G.M.; Ribeiro-Filho, J.; Coutinho, H.D.M.; Pinho, A.I.; Fagner Ferreira Matias, E. Antibiotic-Modifying Activity and Chemical Profile of the Essential Oil from the Leaves of *Cordia verbenacea* DC. *J. Essent. Oil Bear. Plants* **2017**, *20*. [[CrossRef](#)]
16. Matias, E.F.F.; Alves, E.F.; Silva, M.K.N.; Carvalho, V.R.A.; Medeiros, C.R.; Santos, F.A.V.; Bitu, V.C.N.; Souza, C.E.S.; Figueredo, F.G.; Boligon, A.A.; et al. Potentiation of antibiotic activity of aminoglycosides by natural products from *Cordia verbenacea* DC. *Microb. Pathog.* **2016**, *95*, 111–116. [[CrossRef](#)]
17. Costa De Oliveira, D.M.; Luchini, A.C.; Seito, L.N.; Gomes, J.C.; Crespo-López, M.E.; Di Stasi, L.C. *Cordia verbenacea* and secretion of mast cells in different animal species. *J. Ethnopharmacol.* **2011**, *135*, 463–468. [[CrossRef](#)]
18. Parisotto, E.B.; Michielin, E.M.Z.; Biscaro, F.; Ferreira, S.R.S.; Filho, D.W.; Pedrosa, R.C. The antitumor activity of extracts from *Cordia verbenacea* D.C. obtained by supercritical fluid extraction. *J. Supercrit. Fluids* **2012**. [[CrossRef](#)]
19. Ticli, F.K.; Hage, L.I.S.; Cambraia, R.S.; Pereira, P.S.; Magro, Â.J.; Fontes, M.R.M.; Stábeli, R.G.; Giglio, J.R.; França, S.C.; Soares, A.M.; et al. Rosmarinic acid, a new snake venom phospholipase A2 inhibitor from *Cordia verbenacea* (Boraginaceae): Antiserum action potentiation and molecular interaction. *Toxicon* **2005**, *46*, 318–327. [[CrossRef](#)]

20. Missouri Botanical Garden Tropicos Database. 2018. Available online: <http://tropicos.org> (accessed on 20 September 2019).
21. Luzuriaga-Quichimbo, C.X. Estudio Etnobotánico en Comunidades Kichwas Amazónicas de Pastaza, Ecuador. Doctoral Thesis, Universidad de Extremadura, Badajoz, España, 2017. Available online: <http://dehesa.unex.es/handle/10662/6419> (accessed on 10 September 2018).
22. Dos Santos, R.F.E.P.; Silva Silva, I.S.D.M.; d'Costa, L.R.; Mendonça Barbosa, A.; Santos Silva, K.; Ribeiro Amorim, M.; Mendonça Diz, F.; Honório Lins, T.; Santos Sales Verissimo, R.C.; Ferreira Padilha, F.; et al. Study of antimicrobial potential and cytotoxic of *Cordia nodosa* species. *BMC Proc.* **2014**, *8*, P69. [[CrossRef](#)]
23. De La Torre, L.; Navarrete, H.; Muriel, M.P.; Macía, M.J.; Balslev, H. *Enciclopedia de las Plantas Útiles del Ecuador*; Herbario QCA de la Escuela de Ciencias Biológicas de la Pontificia Universidad Católica del Ecuador & Herbario AAU del Departamento de Ciencias Biológicas de la Universidad de Aarhus: Aarhus, Denmark, 2008; ISBN 978-9978-77-135-8.
24. OMS Organización Mundial de la Salud Datos y Cifras Situación Mundial Desafíos a la Producción de Antídotos. Available online: <https://www.who.int/es/news-room/fact-sheets/detail/snakebite-envenoming> (accessed on 10 September 2019).
25. Convention on Biological Diversity. 2010 CoP10 Decisions. 2010; pp. 1–7. Available online: <https://www.cbd.int/decisions/cop/?m=cop-10> (accessed on 10 September 2019).
26. De Filippis, R.; Maina, S.L.; Crepin, J. *Medicinal plants of the Guianas (Guyana, Surinam, French Guiana)*; Department of Botany, National Museum of Natural History, Smithsonian Institution: Washington, DC, USA, 2004.
27. Valadeau, C.; Castillo, J.A.; Sauvain, M.; Lores, A.F.; Bourdy, G. The rainbow hurts my skin: Medicinal concepts and plants uses among the Yanesha (Amuesha), an Amazonian Peruvian ethnic group. *J. Ethnopharmacol.* **2010**, *127*, 175–192. [[CrossRef](#)]
28. Guimaraes, C.; Moreira-Dill, L.; Fernandes, R.; Costa, T.; Hage-Melim, L.; Marcussi, S.; Carvalho, B.; Silva, S.; Zuliani, J.; Fernandes, C.; et al. Biodiversity as a Source of Bioactive Compounds Against Snakebites. *Curr. Med. Chem.* **2014**. [[CrossRef](#)] [[PubMed](#)]
29. Salvador, G.H.; Dos Santos, J.I.; Lomonte, B.; Fontes, M.R. Crystal structure of a phospholipase A2 from *Bothrops asper* venom: Insights into a new putative “myotoxic cluster”. *Biochimie* **2017**, *133*, 95–102. [[CrossRef](#)] [[PubMed](#)]
30. Feliciano, P.R.; Rustiguel, J.K.; Soares, R.O.; Sampaio, S.V.; Cristina Nonato, M. Crystal structure and molecular dynamics studies of L-amino acid oxidase from *Bothrops atrox*. *Toxicon* **2017**, *128*, 50–59. [[CrossRef](#)] [[PubMed](#)]
31. dos Santos, J.I.; Soares, A.M.; Fontes, M.R. Comparative structural studies on Lys49-phospholipases A(2) from *Bothrops* genus reveal their myotoxic site. *J. Struct. Biol.* **2009**, *167*, 106–116. [[CrossRef](#)] [[PubMed](#)]
32. Salvador, G.H.M.; Dreyer, T.R.; Gomes, A.A.S.; Cavalcante, W.L.G.; Dos Santos, J.I.; Gandin, C.A.; de Oliveira Neto, M.; Gallacci, M.; Fontes, M.R.M. Structural and functional characterization of suramin-bound MjTX-I from *Bothrops moojeni* suggests a particular myotoxic mechanism. *Sci. Rep.* **2018**, *8*, 10317. [[CrossRef](#)]
33. Cardoso, F.F.; Borges, R.J.; Dreyer, T.R.; Salvador, G.H.M.; Cavalcante, W.L.G.; Pai, M.D.; Gallacci, M.; Fontes, M.R.M. Structural basis of phospholipase A2-like myotoxin inhibition by chicoric acid, a novel potent inhibitor of ophidian toxins. *Biochim. Biophys. Acta Gen. Subj.* **2018**, *1862*, 2728–2737. [[CrossRef](#)]
34. Watanabe, L.; Soares, A.M.; Ward, R.J.; Fontes, M.R.; Arni, R.K. Structural insights for fatty acid binding in a Lys49-phospholipase A (2): Crystal structure of myotoxin II from *Bothrops moojeni* complexed with stearic acid. *Biochimie* **2005**, *87*, 161–167. [[CrossRef](#)]
35. Ullah, A.; Souza, T.A.; Abrego, J.R.; Betzel, C.; Murakami, M.T.; Arni, R.K. Structural insights into selectivity and cofactor binding in snake venom L-amino acid oxidases. *Biochem. Biophys. Res. Commun.* **2012**, *421*, 124–128. [[CrossRef](#)]
36. Magro, A.J.; Takeda, A.A.; Soares, A.M.; Fontes, M.R. Structure of BthA-I complexed with p-bromophenacyl bromide: Possible correlations with lack of pharmacological activity. *Acta Crystallogr. Sect. D* **2005**, *61*, 1670–1677. [[CrossRef](#)]

37. Marchi-Salvador, D.P.; Correa, L.C.; Magro, A.J.; Oliveira, C.Z.; Soares, A.M.; Fontes, M.R. Insights into the role of oligomeric state on the biological activities of crotoxin: Crystal structure of a tetrameric phospholipase A2 formed by two isoforms of crotoxin B from *Crotalus durissus terrificus* venom. *Proteins* **2008**, *72*, 883–891. [[CrossRef](#)]
38. Lee, W.H.; Da Silva Giotto, M.T.; Marangoni, S.; Toyama, M.H.; Polikarpov, I.; Garratt, R.C. Structural Basis for Low Catalytic Activity in Lys49 Phospholipases A2-A Hypothesis: The Crystal Structure of Piratoxin II Complexed to Fatty Acid. *Biochemistry* **2001**, *40*, 28. [[CrossRef](#)] [[PubMed](#)]
39. Muniz, J.R.; Ambrosio, A.L.; Selistre-de-Araujo, H.S.; Cominetti, M.R.; Moura-da-Silva, A.M.; Oliva, G.; Garratt, R.C.; Souza, D.H. The three-dimensional structure of bothropasin, the main hemorrhagic factor from *Bothrops jararaca* venom: Insights for a new classification of snake venom metalloprotease subgroups. *Toxicon* **2008**, *52*, 807–816. [[CrossRef](#)] [[PubMed](#)]
40. Lingott, T.J.; Schleberger, C.; Gutierrez, J.M.; Merfort, I. High-Resolution Crystal Structure of the Snake Venom Metalloproteinase Bap1 Complexed with a Peptidomimetic: Insight Into Inhibitor Binding. *Biochemistry* **2009**, *48*, 6166. [[CrossRef](#)] [[PubMed](#)]
41. Kumar, J.V.; Chien, K.Y.; Lin, C.C.; Chiang, L.C.; Lin, T.H.; Wu, W.G. Crystal Structure of L-Amino Acid Oxidase from *Naja Atra* (Taiwan Cobra). Available online: <https://www.rcsb.org/structure/5Z2G> (accessed on 13 November 2019).
42. Gergiova, D.; Murakami, M.T.; Perbandt, M.; Arni, R.K.; Betzel, C. Structure of Native L-amino Acid Oxidase from *Vipera ammodytes* Ammodytes: Stabilization of the Quaternary Structure by Divalent Ions and Structural Changes in the Dynamic Active Site. Available online: <https://www.rcsb.org/structure/3KVE> (accessed on 13 November 2019).
43. Lin, C.C.; Wu, B.S.; Wu, W.G. Crystal Structure of Snake Venom Phosphodiesterase (PDE) from Taiwan Cobra (*Naja atra atra*). Available online: <http://dx.doi.org/10.2210/PDB5GZ4/PDB> (accessed on 13 November 2019).
44. Trabi, M.; Millers, E.-K.; Richards, R.; Snelling, H.; Keegan, R.; Lavin, M.F.; de Jersey, J.; Guddat, L.W.; Masci, P. Mechanistic Studies on the Anticoagulant Activity of a Phospholipase A2 from the Venom of the Australian King Brown Snake (*Pseudechis australis*). Available online: <https://www.rcsb.org/structure/3V9M> (accessed on 13 November 2019).
45. Fremont, D.H.; Anderson, D.H.; Wilson, I.A.; Dennis, E.A.; Xuong, N.H. Crystal structure of phospholipase A2 from Indian cobra reveals a trimeric association. *Proc. Natl. Acad. Sci. USA* **1993**, *90*, 342–346. [[CrossRef](#)]
46. Zhang, H.; Teng, M.; Niu, L.; Wang, Y.; Wang, Y.; Liu, Q.; Huang, Q.; Hao, Q.; Dong, Y.; Liu, P. Purification, partial characterization, crystallization and structural determination of AHP-LAAO, a novel L-amino-acid oxidase with cell apoptosis-inducing activity from *Agkistrodon halys pallas* venom. *Acta Crystallogr. Sect. D Biol. Crystallogr.* **2004**, *60*, 974–977. [[CrossRef](#)]
47. Lin, C.C.; Wu, B.S.; Wu, W.G. Crystal Structure of Snake Venom Phosphodiesterase (PDE) from Taiwan Cobra (*Naja atra atra*) in Complex with AMP. Available online: <https://www.rcsb.org/structure/5GZ5> (accessed on 13 November 2019).
48. Segelke, B.W.; Nguyen, D.; Chee, R.; Xuong, N.H.; Dennis, E.A. Structures of two novel crystal forms of *Naja naja naja* phospholipase A2 lacking Ca²⁺ reveal trimeric packing. *J. Mol. Biol.* **1998**, *279*, 223–232. [[CrossRef](#)]
49. Mendes, M.M.; Vieira, S.A.P.B.; Gomes, M.S.R.; Paula, V.F.; Alcântara, T.M.; Homs-Brandeburgo, M.I.; Dos Santos, J.I.; Magro, A.J.; Fontes, M.R.M.; Rodrigues, V.M. Triacetyl p-coumarate: An inhibitor of snake venom metalloproteinases. *Phytochemistry* **2013**. [[CrossRef](#)] [[PubMed](#)]
50. Laskowski, R.A.; Swindells, M.B. LigPlot+: Multiple ligand-protein interaction diagrams for drug discovery. *J. Chem. Inf. Model.* **2011**. [[CrossRef](#)] [[PubMed](#)]
51. Alcaraz, M.J.; Hoult, J.R. Effects of hypolaetin-8-glucoside and related flavonoids on soybean lipoxygenase and snake venom phospholipase A2. *Arch. Int. Pharmacodyn. Ther.* **1985**, *278*, 4–12. [[PubMed](#)]
52. Girish, K.S.; Kemparaju, K. Inhibition of *Naja naja* venom hyaluronidase: Role in the management of poisonous bite. *Life Sci.* **2006**, *78*, 1433–1440. [[CrossRef](#)]
53. Nishijima, C.M.; Rodrigues, C.M.; Silva, M.A.; Lopes-Ferreira, M.; Vilegas, W.; Hiruma-Lima, C.A. Anti-hemorrhagic activity of four brazilian vegetable species against *Bothrops jararaca* venom. *Molecules* **2009**, *14*, 172–180. [[CrossRef](#)]
54. Moher, D.; Liberati, A.; Tetzlaff, J.; Altman, D.G.; PRISMA Group. Preferred reporting items for systematic reviews and meta-analyses: The PRISMA statement. *Int. J. Surg.* **2010**. [[CrossRef](#)]

55. Tu, M.; Cheng, S.; Lu, W.; Du, M. Advancement and prospects of bioinformatics analysis for studying bioactive peptides from food-derived protein: Sequence, structure, and functions. *TrACTrends Anal. Chem.* **2018**. [[CrossRef](#)]
56. Tu, M.; Wang, C.; Chen, C.; Zhang, R.; Liu, H.; Lu, W.; Jiang, L.; Du, M. Identification of a novel ACE-inhibitory peptide from casein and evaluation of the inhibitory mechanisms. *Food Chem.* **2018**. [[CrossRef](#)]



© 2019 by the authors. Licensee MDPI, Basel, Switzerland. This article is an open access article distributed under the terms and conditions of the Creative Commons Attribution (CC BY) license (<http://creativecommons.org/licenses/by/4.0/>).